nature cell biology

Identification and characterization of a non-satellite cell muscle resident progenitor during postnatal development

Kathryn J. Mitchell[1,2], Alice Pannérec[1,2], Bruno Cadot[1,3], Ara Parlakian[1,2], Vanessa Besson[1,2], Edgar R. Gomes[1,3], Giovanna Marazzi[1,2,4] and David A. Sassoon[1,2,4,5]

Satellite cells are resident myogenic progenitors in postnatal skeletal muscle involved in muscle postnatal growth and adult regenerative capacity. Here, we identify and describe a population of muscle-resident stem cells, which are located in the interstitium, that express the cell stress mediator PW1 but do not express other markers of muscle stem cells such as Pax7. PW1$^+$/Pax7$^-$ interstitial cells (PICs) are myogenic *in vitro* and efficiently contribute to skeletal muscle regeneration *in vivo* as well as generating satellite cells and PICs. Whereas Pax7 mutant satellite cells show robust myogenic potential, Pax7 mutant PICs are unable to participate in myogenesis and accumulate during postnatal growth. Furthermore, we found that PICs are not derived from a satellite cell lineage. Taken together, our findings uncover a new and anatomically identifiable population of muscle progenitors and define a key role for Pax7 in a non-satellite cell population during postnatal muscle growth.

Postnatal skeletal muscle growth and regeneration is dependent on muscle-resident progenitor cells[1–9]. Considerable work has demonstrated that satellite cells are a major source of progenitor cells in postnatal skeletal muscle[2,5,6,8,10–13]. Satellite cells were first defined by their anatomical location between the basal lamina and muscle fibre plasma membrane[14]. The identification of genes specifically expressed in satellite cells, such as the paired box transcription factor, *Pax7* (ref. 8) and MCadherin[15], allows for their identification using standard microscopy. Pax7 is required for postnatal muscle growth and maintenance of the satellite cell population, and both Pax3 and Pax7 participate in the establishment of the myogenic lineage during early development[12,16]. Constitutive Pax7 mutant muscle shows a significant reduction in the satellite cell population during the first weeks of postnatal life, which is attributed to decreased proliferative capacity[17–19] and increased apoptosis[19]. Studies using primary muscle culture and isolated single myofibres support a role for Pax7 in satellite cell self-renewal[13,20,21]. A recent report demonstrated that Pax7 and Pax3 are not required during adult life[22], suggesting that key cellular events during postnatal muscle development remain to be elucidated.

Non-satellite cell progenitors, such as bone marrow-derived circulating stem cells and muscle resident cell populations, can also participate in myogenesis[23–26]. However, as a consequence of the methods used to isolate these myogenic progenitors, such as cell culture selection techniques and flow cytometry-based sorting using cell surface markers or Hoechst dye exclusion, critical information is missing regarding the precise anatomical localization of these non-satellite cell progenitors, as well as their physiological contribution to muscle growth and repair[23,24,26–29], with the exception of mesoangioblasts, which can be localized as alkaline phosphatise-positive cells associated with the vessels[30].

We used a differential screening approach to identify factors involved in skeletal muscle stem cell commitment leading to the isolation of PW1/Peg3 (ref. 31). PW1 is expressed in primary myoblasts and myogenic cell lines[31–34]. PW1 expression initiates in early embryonic mesoderm and is downregulated in tissues as they differentiate[31]. In postnatal skeletal muscle, PW1 expression is detected in satellite cells and a subset of interstitial cells and is markedly upregulated during muscle regeneration[32,33]. PW1 participates in TNF–NFκB signalling and p53-mediated cell stress pathways[32–37]. Transgenic mice expressing a truncated form of PW1 (ΔPW1) that inhibits TNF and p53 signalling pathways[5] show a profound failure in postnatal muscle growth reminiscent of the Pax7 constitutive mutant phenotype[8,33]. ΔPW1-expressing mice are severely atrophic despite the presence of active Pax7$^+$ cell clusters underneath the basal lamina, implicating a role for PW1 in stem cell behaviour and postnatal muscle growth[33]. Together with p53, PW1 participates in regulating intrinsic and extrinsic stress pathways in myoblasts, placing PW1 as a key regulator of muscle atrophy[32,35].

In this study, we show that PICs can be isolated and their cell fate determined. PICs show bipotential behaviour *in vitro,* generating both smooth and skeletal muscle. Using single cell analyses, we observed that both lineages can be derived from a single PIC. Whereas freshly isolated

[1,2,3]Myology Group, [2]Stem Cell and Muscle Biology, [3]Cytoskeleton Architecture and Cell Polarization, UMR S 787 INSERM, Université Pierre et Marie Curie Paris VI, Paris, 75634, France. [4]Co-senior authors.
[5]Correspondence should be addressed to D.A.S. (e-mail: david.a.sassoon@gmail.com).

Received 17 November 2009; accepted 14 January 2010; published online 31 January 2010; DOI: 10.1038/ncb2025

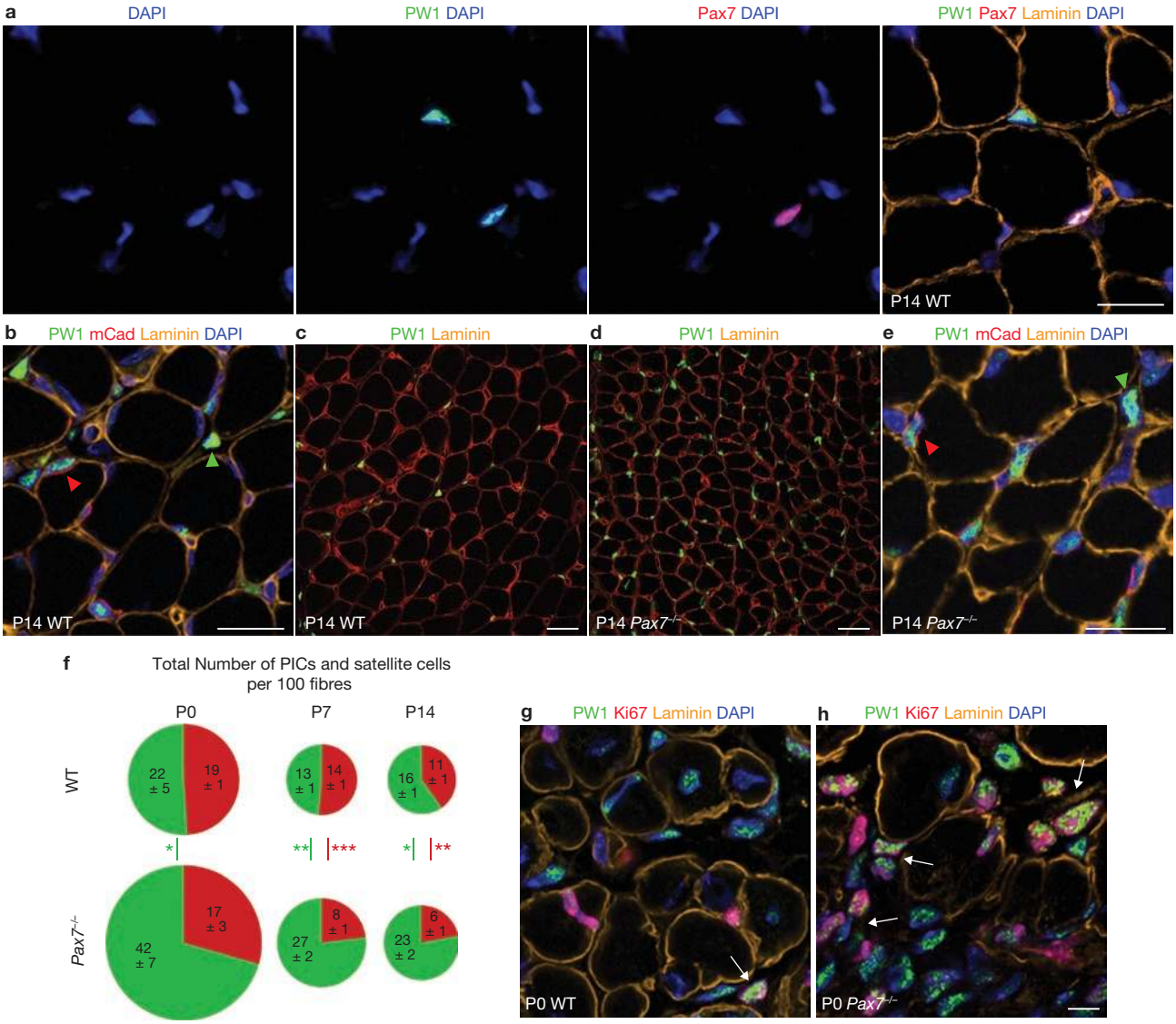

Figure 1 PW1 identifies two distinct populations in postnatal muscle under the regulation of Pax7. (**a**) Cross-section of a P14 hindlimb muscle immunostained for PW1 (green) and Pax7 (red) to identify satellite cells. Laminin staining (orange) shows the basal lamina. Nuclei were counterstained by DAPI (blue). We note that PW1 is expressed in satellite cells (colocalized with Pax7) in addition to a subset of interstitial cells (Pax7-negative). Scale bar, 50 μm. (**b**) Cross-section of a P14 hindlimb muscle from wild-type (P14 WT) mice immunostained for PW1 (green), mCadherin (red) to identify satellite cells and laminin (orange). DAPI staining identifies nuclei (blue). We note PW1 is expressed in satellite cells (mCadherin-positive, red arrowhead) and in a subset of interstitial cells that do not express mCadherin (green arrowhead). Scale bar, 50 μm. (**c**, **d**) Cross-sections of P14 hindlimb muscles from wild-type (P14 WT; **c**) and Pax7$^{-/-}$ (P14 *Pax7*$^{-/-}$; **d**) mice immunostained for PW1 (green) and laminin (red). The number of PW1^{+} cells is markedly increased in Pax7$^{-/-}$ muscle. Scale bars, 100 μm. (**e**) Cross-section of Pax7$^{-/-}$ P14 hindlimb muscle (P14 *Pax7*$^{-/-}$) immunostained for mCadherin (red), PW1 (green) and laminin (orange). DAPI staining (blue) identifies nuclei. Satellite cells (red arrowhead) and PICs (green arrowhead) are readily identified. Scale bar, 50 μm. (**f**) Quantification of PICs (green) and satellite cells (red) per 100 fibres for wild-type and *Pax7*$^{-/-}$ mice at P0, P7 and P14 from cross-sections immunostained as shown in **b** and **e**. Values represent the mean number of positive cells ± s.e.m. per 100 fibres and statistical analyses were performed using Student's *t*-test, $*P < 0.05$, $**P < 0.01$ and $***P < 0.001$ ($n = 4$ per genotype and age). Circle area is relative to the total cell number. In *Pax7*$^{-/-}$ muscle, the number of PICs is significantly increased at all stages examined. (**g**, **h**) Cross-sections of P0 hindlimb muscles from wild-type (P0 WT) and *Pax7*$^{-/-}$ (P0 *Pax7*$^{-/-}$) mice immunostained for Ki67 (red), to identify proliferating cells, PW1 (green) and laminin (orange). Wild-type and *Pax7*$^{-/-}$ PICs express Ki67 (proliferation marker, arrows). We note clusters of proliferating PICs in *Pax7*$^{-/-}$ muscle only. Scale bar, 50 μm.

PICs do not express Pax7 or MyoD, we observed that they convert to a Pax7^{+}/MyoD^{+} state before forming skeletal muscle *in vitro*. Furthermore, we detected pronounced myogenic capacity of PICs following injection into damaged muscle tissue *in vivo*, comparable to that observed with freshly isolated satellite cells. Pax7 mutant mice (*Pax7*$^{-/-}$) show a marked increase in PICs during postnatal development, which is inversely proportional to the decrease in satellite cells. Satellite cells isolated from *Pax7*$^{-/-}$ mice proliferate well and are highly myogenic *in vitro*, however, *Pax7*$^{-/-}$ PICs show almost no skeletal myogenic capacity but retain the ability to become smooth muscle. Using lineage analyses, we show that PICs are not derived from a Pax3-expressing parental cell and thus do not share a satellite cell lineage; however, PICs do express Pax3 upon conversion to skeletal muscle. These data identify a new bipotent resident stem cell in skeletal muscle and are consistent with a model whereby Pax7

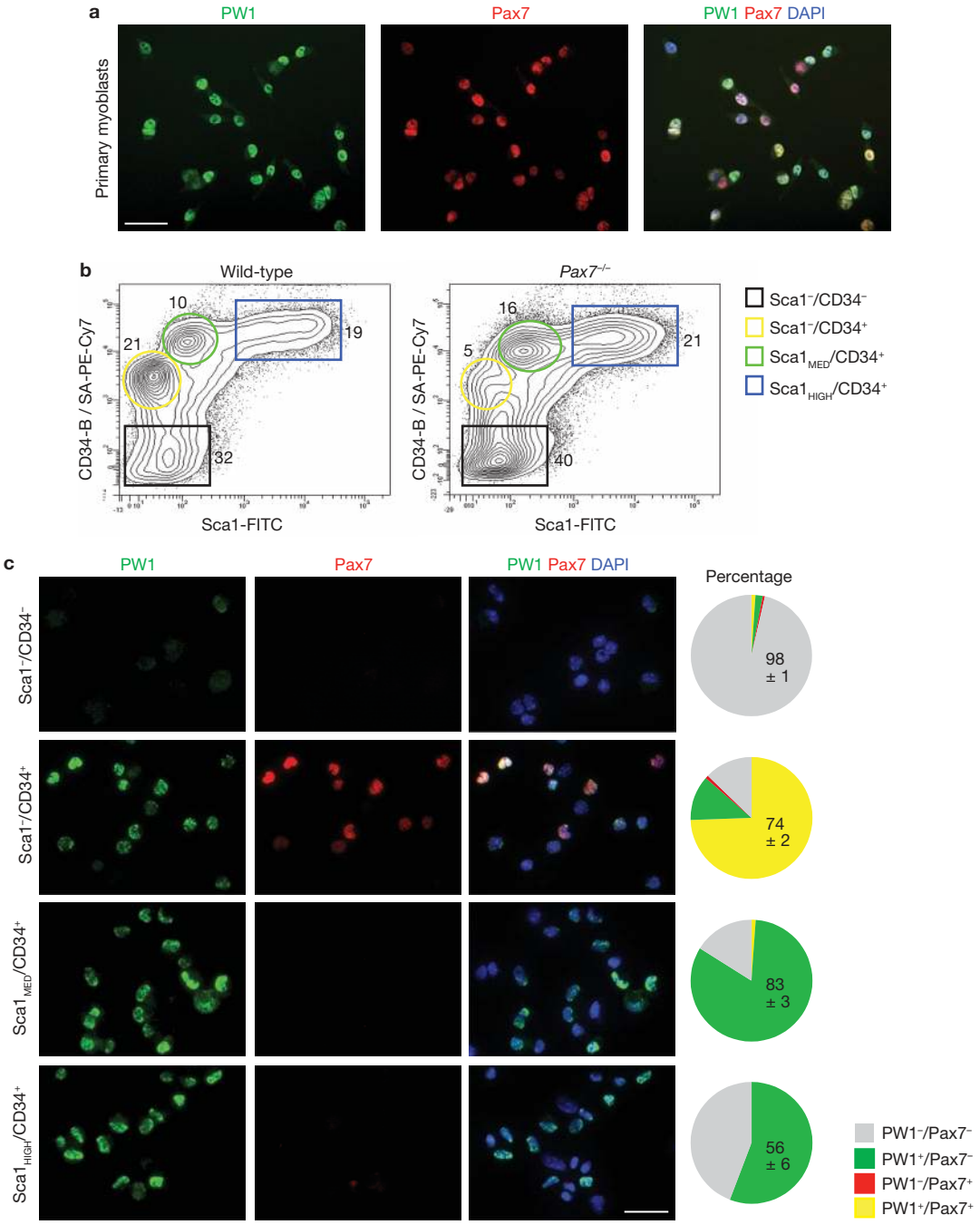

Figure 2 PICs are enriched in the muscle-resident Sca1$^+$/CD34$^+$ population. (**a**) Proliferating primary bulk muscle cultures immunostained for PW1 (green) and Pax7 (red) show co-expression of both genes. Nuclei were counterstained with DAPI (blue). PW1-expressing cells that do not express Pax7 cannot be identified *in vitro*. Scale bar, 30 μm. (**b**) Flow cytometric analyses of single cells from P10 hindlimb muscles from wild-type or *Pax7*$^{-/-}$ mice stained with antibodies against Sca1 and CD34. CD45$^+$ and Ter119$_{HIGH}$ cells were excluded as described in Supplementary Information, Fig. S1. The gates used to isolate Sca1$^-$/CD34$^-$, Sca1$^-$/CD34$^+$, Sca1$_{MED}$/CD34$^+$ and Sca1$_{HIGH}$/CD34$^+$ cells are shown. The four fractions are indicated directly on the scatterplot. Values represent the mean percentage of the parent population from four independent experiments. (**c**) Immunolocalization of PW1 (green) and Pax7 (red) in freshly sorted cytospun cell fractions, as shown in **b**. Nuclei are shown by DAPI staining (blue). PW1$^+$/Pax7$^+$ cells are in the Sca1$^-$/CD34$^+$ fraction and PW1$^+$/Pax7$^-$ cells are in the Sca1$^+$/CD34$^+$ fraction. Quantification of the staining (far right) shows that the Sca1$_{MED}$/CD34$^+$ population is highly enriched in PW1$^+$/Pax7$^-$ cells (PICs). Values are presented as the mean percentage ± s.e.m., $n = 5$. Scale bar, 30 μm.

expression is required for the postnatal recruitment of PICs to skeletal muscle during postnatal growth. Furthermore, these data implicate PICs as a key cell population that cannot be recruited into the skeletal muscle lineage in the absence of Pax7 function and is likely to contribute to the Pax7 muscle phenotype during postnatal growth.

RESULTS

PW1 identifies two distinct populations in postnatal muscle

To define the cell types in which PW1 is expressed in postnatal muscle, we stained muscle tissue sections for PW1, laminin to delineate the basal lamina and Pax7 (Fig. 1a) or MCadherin[15] (Fig. 1b) to identify satellite

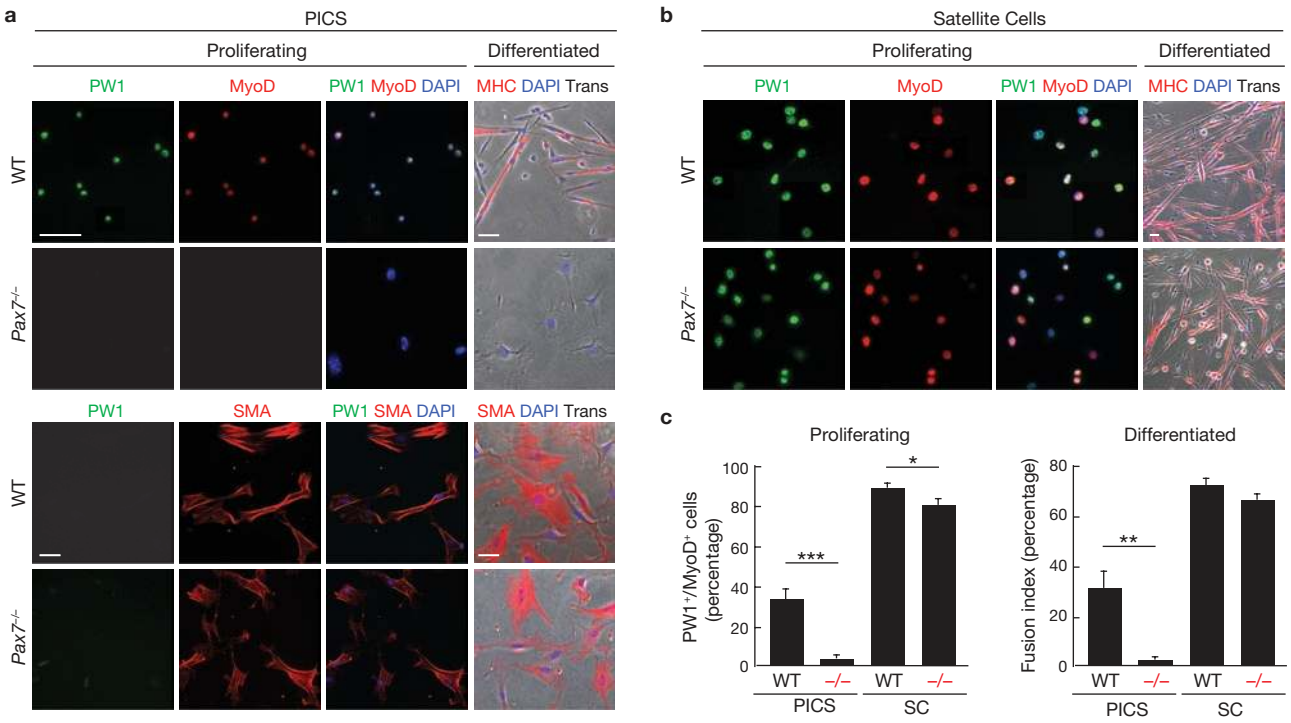

Figure 3 PICs spontaneously convert to skeletal myogenic cells via a Pax7-dependent pathway. (**a**) Top panels: myogenic cells were identified in cultures of proliferating wild-type and *Pax7*$^{-/-}$ PICs by immunostaining for PW1 (green) and MyoD (red). After 32 h in differentiation medium (Differentiated, far right), wild-type and *Pax7*$^{-/-}$ PICs were immunostained for myosin heavy chain (MHC; red) to determine biochemical differentiation. Bottom panels: immunolocalization of PW1 (green) and smooth muscle actin (SMA; red) in proliferating and differentiated wild-type and *Pax7*$^{-/-}$ PICs. Nuclei were counterstained with DAPI. Cultured PICs that express smooth muscle actin lose their PW1 expression. We note that whereas wild-type PICs acquire both myogenic and smooth muscle phenotypes, *Pax7*$^{-/-}$ PICs almost exclusively become smooth muscle. Under these conditions, only MyoD-negative cells express smooth muscle actin (Supplementary Information, Fig. S1). Scale bars, 50 μm. (**b**) Representative photomicrographs of proliferating wild-type and *Pax7*$^{-/-}$ satellite cells immunostained for PW1 (green) and MyoD (red). After 32 h in differentiating medium (Differentiated, far right), wild-type and *Pax7*$^{-/-}$ satellite cells were immunostained for myosin heavy chain (MHC; red). Nuclei are shown by DAPI. Note that *Pax7*$^{-/-}$ satellite cells are myogenically competent. Scale bar, 50 μm. (**c**) Quantitative analysis of myogenic competence and differentiation of cells treated as described in **a** and **b**. Proliferating values represent the mean percentage ± s.e.m. of proliferating cells co-expressing MyoD and PW1. Differentiated values show the mean percemtage ± s.e.m. of nuclei incorporated into MHC^{+} cells. *Pax7*$^{-/-}$ satellite cells are as myogenic as wild-type satellite cells. *Pax7*$^{-/-}$ PICS in culture lose PW1 expression, do not express MyoD and do not differentiate into skeletal muscle. $n = 5$ for each assay and genotype.

cells. Interstitial PW1^{+}/Pax7^{-} cells are abundant at birth, remain identifiable into adult life and then decline in older muscle, but increase following muscle injury (data not shown)[32,33,35]. As *Pax7*$^{-/-}$ mice have a significantly reduced lifespan[8,17,38], we restricted our analyses to the first 2 weeks of postnatal development. We observed that PW1 was expressed in two distinct compartments: satellite cells and a subset of interstitial cells (Fig. 1a, b)[32,33]. Most satellite cells expressed PW1 at postnatal day (P) 14 (93 ± 4%; $n = 3$ mice, > 350 fibres per mouse). PW1 expression was also detected in a subpopulation of interstitial cells (23 ± 3%; $n = 3$ mice, > 350 fibres per mouse). PICs did not express skeletal muscle, smooth muscle, endothelial or macrophage-specific gene markers at detectable levels, however, PICs were positive for vimentin (Supplementary Information, Fig. 1a–e), characteristic of muscle progenitors[39,40].

The PIC population is markedly increased in Pax7 mutant muscle

As the satellite cell compartment is reduced in the *Pax7*$^{-/-}$ mouse[8], we predicted that overall levels of PW1^{+} cells would decrease, reflecting the decrease in satellite cells. Surprisingly, we observed a marked increase in PW1^{+} cells in the Pax7 mutant by P14 (Fig. 1c, d). We quantified the number of satellite cells and PICs in wild-type, *Pax7*$^{+/-}$ and *Pax7*$^{-/-}$ muscle during postnatal development (Fig. 1f). We found that *Pax7*$^{+/-}$ muscle showed no significant phenotype, therefore only data from wild-type and *Pax7*$^{-/-}$ mice are presented. We considered MCadherin-positive cells present under the basal lamina to be satellite cells[41–43]. As in wild-type muscle (Fig. 1b), satellite cells and PICs were detected in *Pax7*$^{-/-}$ muscle (Fig. 1e). The percentage of satellite cells expressing PW1 did not vary significantly (93 ± 4% versus 98 ± 2% for wild-type and *Pax7*$^{-/-}$, respectively, at P14; $n = 3$ mice per genotype, > 350 fibres from randomly chosen fields per mouse; see Methods), however, we observed clear differences in the total number and ratio of satellite cells and PICs (Fig. 1f). At birth (P0), wild-type and *Pax7*$^{-/-}$ mice showed similar numbers of satellite cells, however, during postnatal growth (P7 and P14) this population declined significantly in Pax7 mutant mice. In contrast, the number of PICs was significantly elevated in Pax7 mutant mice at all stages examined. The most notable difference was observed at birth where twofold more PICs were present in Pax7 mutant mice (Fig. 1f), resulting in an expansion of the interstitial compartment (39 ± 2 versus 52 ± 6 interstitial cells per 100 fibres for wild-type and *Pax7*$^{-/-}$mice, respectively, at $P = 0$; $n = 3$ mice per genotype, $P = 0.05$, > 350 fibres per mouse). Overall, we observed a shift in the ratio of PICs to satellite cells from ~ 1:1 in wild-type to ~ 3:1 in Pax7 mutant mice (Fig. 1f). The increase in PICs at birth represents the earliest phenotype detectable in *Pax7*$^{-/-}$ muscle, preceding the decline in satellite cell number.

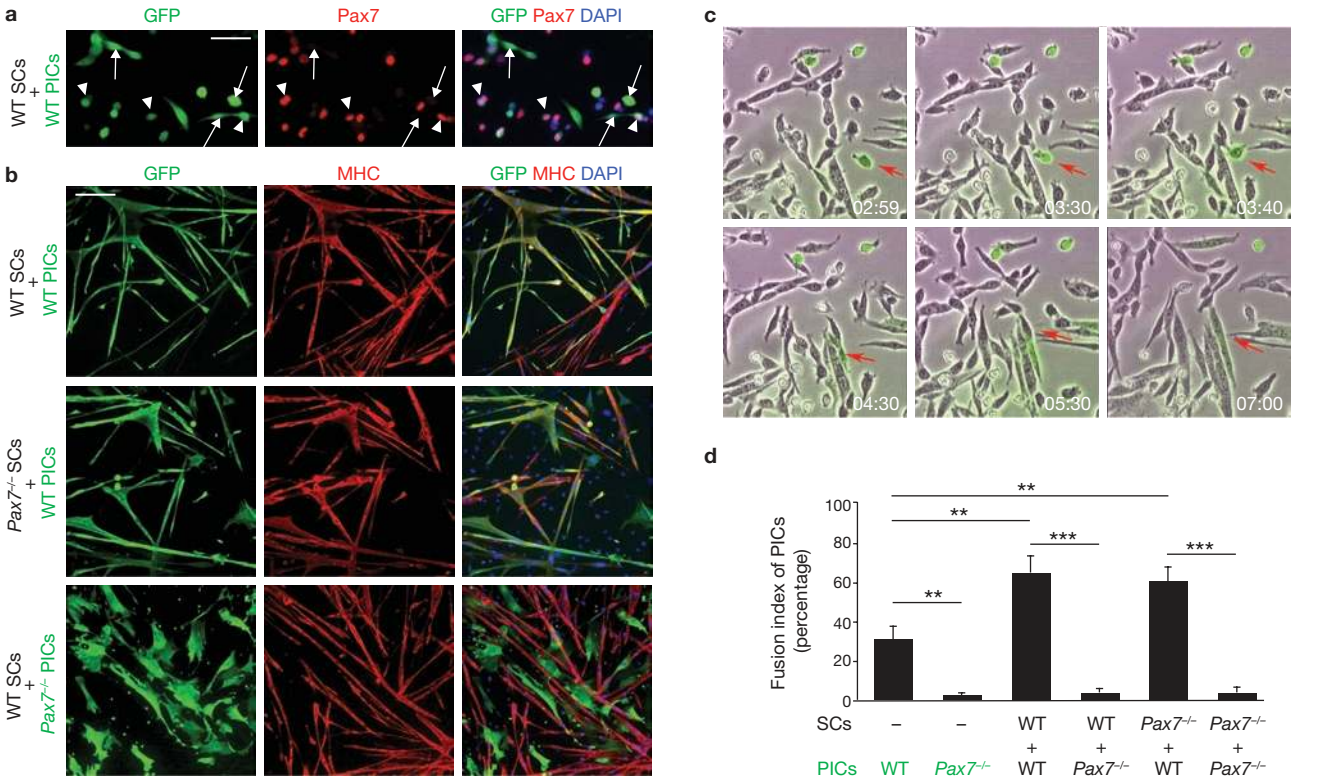

Figure 4 Pax7 is required for PICs to participate in myogenesis. (**a**) GFP-labelled wild-type PICs (WT PICs) grown with wild-type unlabelled satellite cells (WT SCs) for 96 h in growth medium. Immunostaining for GFP and Pax7 shows Pax7-positive GFP-negative satellite cells (red) in close proximity to Pax7-negative GFP-positive PICs (green; arrows) and GFP-positive PICs that have switched on Pax7 (arrowheads). Nuclei were counterstained with DAPI. Scale bar, 50 μm. (**b**) Top Panels, wild-type unlabelled satellite cells (WT SCs) grown in co-culture with WT GFP-labelled PICs (WT PICs) and allowed to differentiate in differentiation medium for 32 h. Immunolocalization of MHC (red) and GFP (green) shows GFP$^+$MHC$^+$ myotubes. Middle Panels, Pax7 mutant unlabelled satellite cells (Pax7$^{-/-}$ SCs) grown with GFP-labelled wild-type PICs (WT PICs) and allowed to differentiate in differentiation medium for 32 h. Immunolocalization of MHC (red) and GFP (green) shows GFP$^+$MHC$^+$ myotubes. Bottom panel, wild-type unlabelled satellite cells (WT SCs) grown in co-culture with wild-type GFP-labelled Pax7 mutant PICs (*Pax7*$^{-/-}$ PICs) and allowed to differentiate in DM for 32 h. No GFP$^+$MHC$^+$ myotubes were observed in co-cultures containing *Pax7*$^{-/-}$ PICs. Nuclei were counterstained with DAPI. Scale bar, 100 μm. (**c**) Frames from a time-lapse recording of co-cultures of wild-type GFP-labelled PICs (green) and wild-type unlabelled satellite cells (see also, Supplementary Information, Movie 1). Cells were transferred to low-serum conditions at time, 0. Time elapsed is shown in h:min. GFP$^+$ PICs readily fuse with satellite cell-derived myoblasts (arrows). (**d**) Quantitative analysis of myogenic differentiation of GFP-labelled PICs grown with unlabelled satellite cells (SCs), as shown in **b**. *Pax7*$^{-/-}$ PICs do not differentiate even when co-cultured with wild-type satellite cells. Values represent the percentage of nuclei in MHC$^+$ cells for GFP$^+$ cells only (mean ± s.e.m., $n = 4$ for each condition).

To determine the proliferative status of PICs, we stained wild-type and *Pax7*$^{-/-}$ muscles at various stages of postnatal development for Ki67. We noted clusters of Ki67$^+$ PICs in *Pax7*$^{-/-}$ at P0, whereas only scattered Ki67$^+$ PICs were observed in the wild-type muscle (Fig. 1g, h), revealing that loss of Pax7 is concomitant with an increase in PIC proliferation. By 1 week after birth, PICs and satellite cells were mitotically quiescent in wild-type muscle with few proliferative cells at birth.

PICs are present in the skeletal muscle Sca1$^+$/CD34$^+$ population

Primary bulk cultures (cultures of all single cells) derived from postnatal muscle gave rise to numerous myogenic cells, all of which co-expressed PW1 and Pax7 following several days in culture (Fig. 2a). In contrast, we never observed PW1$^+$ cells that expressed Pax7 or MyoD in culture, even though PICs were as abundant as satellite cells in muscle tissue (Fig. 1f). As a prerequisite step to explore PIC cell fate, we developed a fluorescence-activated cell sorting (FACS) approach using cell-surface markers previously used to isolate muscle stem cell populations[26,29,44]. Freshly sorted cells from P7–10 pooled muscle were immediately cytospun onto glass slides and analysed for PW1 and Pax7 expression. The Ter119$_{HIGH}$ and CD45$^+$ populations were completely PW1- and Pax7-negative whereas the remaining fraction contained a mixture of PW1$^+$ and PW1$^-$ cells (Supplementary Information, Fig. S1f–h). This fraction was then sorted for Sca1 and CD34, revealing four distinct populations (Fig. 2b; Supplementary Information, Fig. S1f). Satellite cells (PW1$^+$/Pax7$^+$) were present in the Sca1$^-$/CD34$^+$ fraction (Fig. 2c), in agreement with previous studies[2,44]. Upon isolation, PW1$^+$/Pax7$^-$ cells were considered to be PICs, corresponding to the only population of PW1$^+$/Pax7$^-$ cells *in vivo*. These cells were enriched in the two Sca1$^+$/CD34$^+$ fractions (Fig. 2c). As the Sca1$_{MED}$ fraction contained > 80% PICs, this fraction was further investigated *in vitro* and *in vivo*. The same approach was used to isolate satellite cells and PICs from *Pax7*$^{-/-}$ mice. In agreement with our *in vivo* quantification (Fig. 1f), loss of Pax7 resulted in a diminished satellite cell fraction (21 ± 4% for wild-type, 5 ± 1% for Pax7$^{-/-}$; $n = 4$; $P < 0.01$) and a larger Sca1$_{MED}$/CD34$^+$ fraction (10 ± 2% for wild-type and 16 ± 2% for Pax7$^{-/-}$; $n = 4$; $P < 0.05$; Fig. 2b), of which 72 ± 2% were PICs ($n = 3$). Significant changes in other fractions were not observed (Supplementary Information, Fig. S1h).

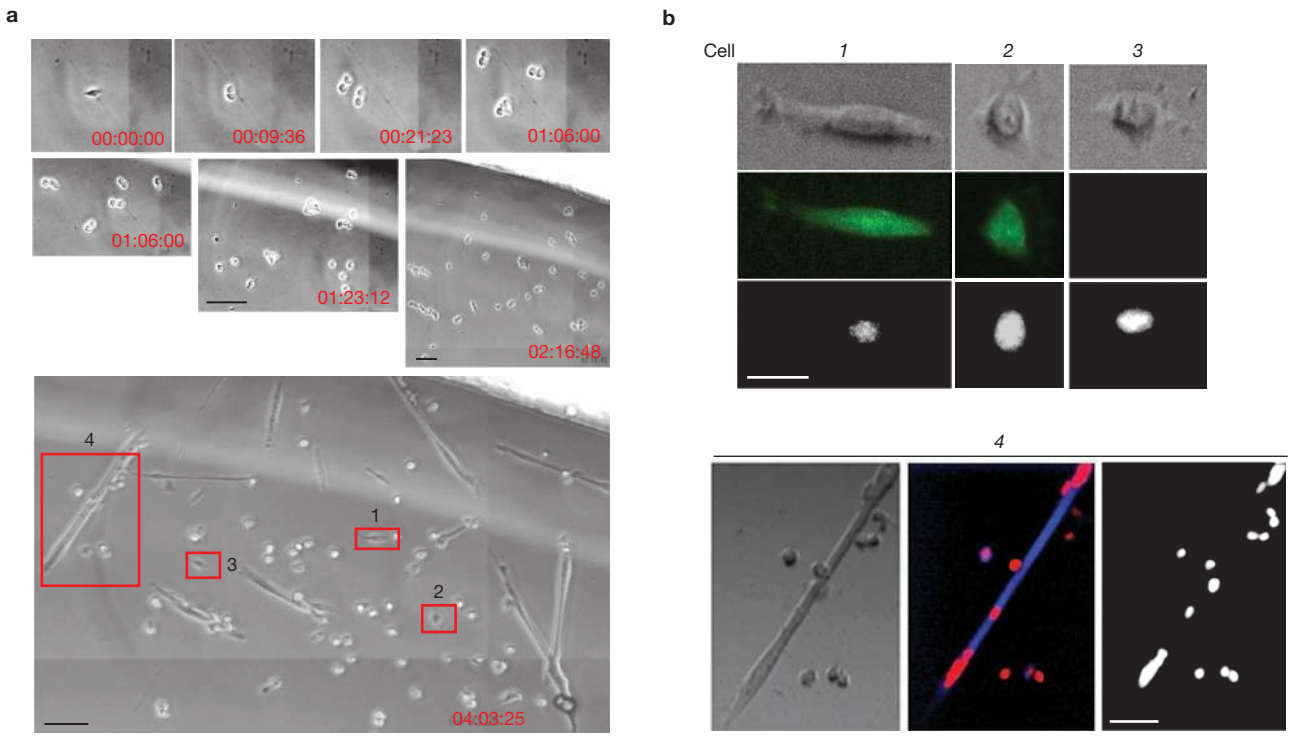

Figure 5 PICs are bipotent and give rise to smooth and skeletal muscle. (**a**) Representative frames from a time-lapse recording of freshly isolated PICs. Cells were observed for 3 days in proliferating medium and 24 h in differentiating medium (time in day:h:min). During this period, cells from different clones did not mix (Supplementary Information, Movie 2). A single cell divides several times during proliferation (from 0:00:00 until 3:00:00). After 24 h in differentiation medium, some of the daughter cells fused to form myotubes (bottom panel). Scale bars, 50 μm for middle panels and 100 μm for bottom panel. (**b**) Immunostaining for SM22 (green) MyoD (red) and MHC (blue) at the end of acquisition (4:03:25) was performed on selected daughter cells shown in the boxed, numbered cells in **a** (bottom panel), and shows lineage differences. The high magnification images show representative outcomes. Two examples of smooth muscle cells (numbers 1 and 2), which are positive for SM22 and negative for MyoD, are shown. We also observed a few cells that were negative for all markers used (number 3) and myotubes as well as single cells positive for MHC and MyoD (number 4). In this experiment, one PIC generated 149 nuclei, of which 117 corresponded to skeletal muscle ($MyoD^+$), 35 corresponded to smooth muscle ($SM22^+/MyoD^-$) and 15 showed no detectable staining. Scale bars, 30μm for top panel and 100 μm for bottom panel.

PICs show pronounced myogenic capacity *in vitro*

Freshly purified PICs were placed in culture to test for myogenic differentiation. After 4 days in culture, ~ 30% of cells were positive for MyoD and PW1 (Fig. 3a), and Pax7 (data not shown) and gave rise to myosin heavy chain (MHC)-expressing multinucleate myotubes after 24 h in differentiation conditions (Fig. 3a). Cells that did not form myotubes did not express skeletal muscle markers nor PW1, however, most expressed smooth muscle actin (Fig. 3a), suggesting that PICs also give rise to smooth muscle. Further analyses revealed that only smooth muscle actin-negative cells were positive for MyoD and PW1 (supplementary Information, Fig. S1i).

Pax7 is required for myogenic specification of PICs

As loss of Pax7 results in a decrease in satellite cells and an increase in PICs (Fig. 1f), we investigated whether loss of Pax7 altered PIC behaviour in culture. PICs and satellite cells from wild-type and *Pax7*$^{-/-}$ mice were purified and directly compared *in vitro*. We observed that wild-type and *Pax7*$^{-/-}$ satellite cells proliferated equally well in culture and that ~ 80% of cells expressed both MyoD and PW1. Furthermore, loss of Pax7 had no impact on the differentiation potential of satellite cells *in vitro* (Fig. 3b, c). The behaviours of wild-type and Pax7 mutant PICs were markedly different. In proliferating cultures, only ~3% of *Pax7*$^{-/-}$ PICs were $MyoD^+/PW1^+$, resulting in a fusion index of ~ 2%, in contrast to > 30% myogenicity of wild-type PICs (Fig. 3a, c). The smooth muscle fate of PICs was unaffected (Fig. 3a).

To investigate whether skeletal myoblasts influence the myogenic potential of PICs, we co-cultured wild-type GFP-labelled PICs with wild-type unlabelled satellite cells, and tracked PICs using GFP as a marker. Under proliferating conditions, we observed PICs that did not express Pax7 in close proximity to PICs that expressed Pax7, together with $Pax7^+$ satellite cells (GFP^-; Fig. 4a). We noted that $GFP^+/Pax7^-$ cells adopted a small, rounded phenotype, suggesting satellite cells alter PIC behaviour *in vitro* (Fig. 4a; Supplementary Information, Fig. S2). In differentiated cultures, > 60% of all nuclei in GFP^+ cells were in myotubes (verified by staining for MHC) compared with ~ 30% in cultures of PICs alone (Fig. 4b, top panels and Fig. 4d). We performed live-cell imaging of differentiating GFP-labelled PICs with unlabelled satellite cells to follow cell interactions over time. We observed that GFP^+ cells (PICs) readily fused with unlabelled myoblasts and myofibres to form fibres composed of both satellite cells and PICs (Fig. 4c; Supplementary Information, Movie 1).

Both wild-type and *Pax7*$^{-/-}$ satellite cells had comparable effects on the myogenic potential of wild-type PICs, revealing that Pax7 is not required by satellite cells to fuse with PICs (Fig. 4b, d). In contrast, *Pax7*$^{-/-}$ PICs were myogenically deficient when co-cultured with satellite cells from either wild-type or *Pax7*$^{-/-}$ mice, giving rise to ~ 3% of nuclei in GFP^+ cells being incorporated into myotubes (Fig. 4b, d). These data demonstrate that Pax7 is required for the myogenic capacity of PICs, whereas loss of Pax7 has little effect on purified satellite cells.

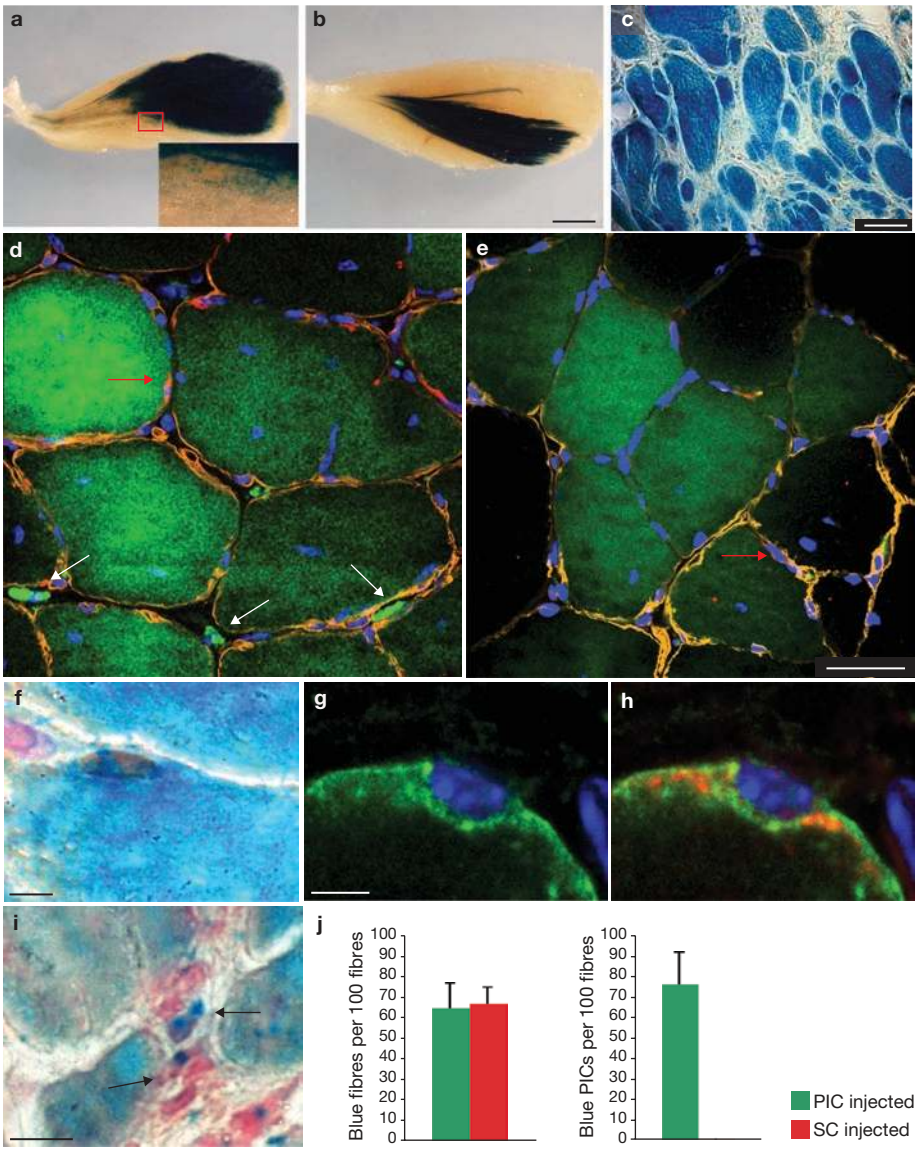

Figure 6 PICs are myogenic and recolonize the PIC niche *in vivo*. (**a**, **b**) Tibialis anterior muscle 2 weeks after injection with either 15,000 PICs (**a**) or satellite cells (**b**) freshly isolated from 10-day-old *R26LacZ* hind- and forelimbs. Muscles were tested for β-galactosidase activity. In PIC-transplanted muscle, LacZ staining is diffuse (see inset). (**c**) Cross-section of the tibialis anterior of nude mice injected with *R26LacZ* PICs as shown in **a**. β-Galactosidase staining (blue) revealed PIC contribution to myofibres and interstitial cells. (**d**, **e**) Representative cross-section of the tibialis anterior of nude mice 2 weeks after injection with 15,000 PICs (**d**) or satellite cells (**e**) freshly isolated from 9-day-old β-actin–EGFP limb muscles. Sections were immunostained for mCadherin (red) and laminin (orange). GFP fluorescence is shown in green. Nuclei were counterstained with DAPI (blue). Interstitial GFP-positive cells are only observed in PIC-transplanted muscles (white arrows). mCadherin labelling is present in GFP-positive fibres corresponding to cells in the satellite cell compartment (red arrows). Scale bar, 50 μm. (**f**) High resolution cross-section of the tibialis anterior injected with *R26LacZ* PICs and immunostained for Pax7 (brown). Scale bar, 10 μm. (**g**, **h**) High resolution cross-section of the tibialis anterior injected with *β-actin–EGFP* PICs and immunostained for GFP (green) and mCadherin (red), showing PIC-derived satellite cells adjacent to a weakly positive GFP fibre. Scale bar, 10 μm. (**i**) High resolution cross-section of tibialis anterior injected with *R26LacZ* PICs and immunostained for PW1 (brown), showing PW1-expressing blue interstitial cells (arrows). Scale bar, 50 μm. (**j**) Left panel, histogram showing the number of blue fibres normalized to fibre number in regenerating areas. We noted that PICs and satellite cells show comparable contributions to muscle fibres following injection. Values represent the mean percentage ± s.e.m. from four independent experiments. Right panel, histogram showing the number of blue interstitial cells per 100 fibres following *R26LacZ* PIC (green bar) and satellite cell (red bar) injection normalized to 100 fibres in regenerating areas. We observed that satellite cells do not generate PICs whereas ~75 PICs per 100 fibres are present following PIC injection. Values represent the mean percentage ± s.e.m. from four independent experiments. At least 250 fibres were counted for each experiment.

PICs are bipotent

The observation that PICs give rise to smooth and skeletal muscle suggests that PICs have two cell fates. We used live-cell imaging of single cell cultured PICs to determine the complete cell fates of resultant daughter cells over the course of 3–4 days under growth conditions followed by 24 h of differentiation. We followed the division and movements of single and daughter cells (Fig. 5a; Supplementary Information, Fig. S2 and Movie 2). As shown in Fig. 5, single PICs gave rise to daughter cells that acquired both skeletal and smooth muscle fates, as determined by staining for MyoD, MHC and SM22 (Fig. 5b). We did not see mixed cell

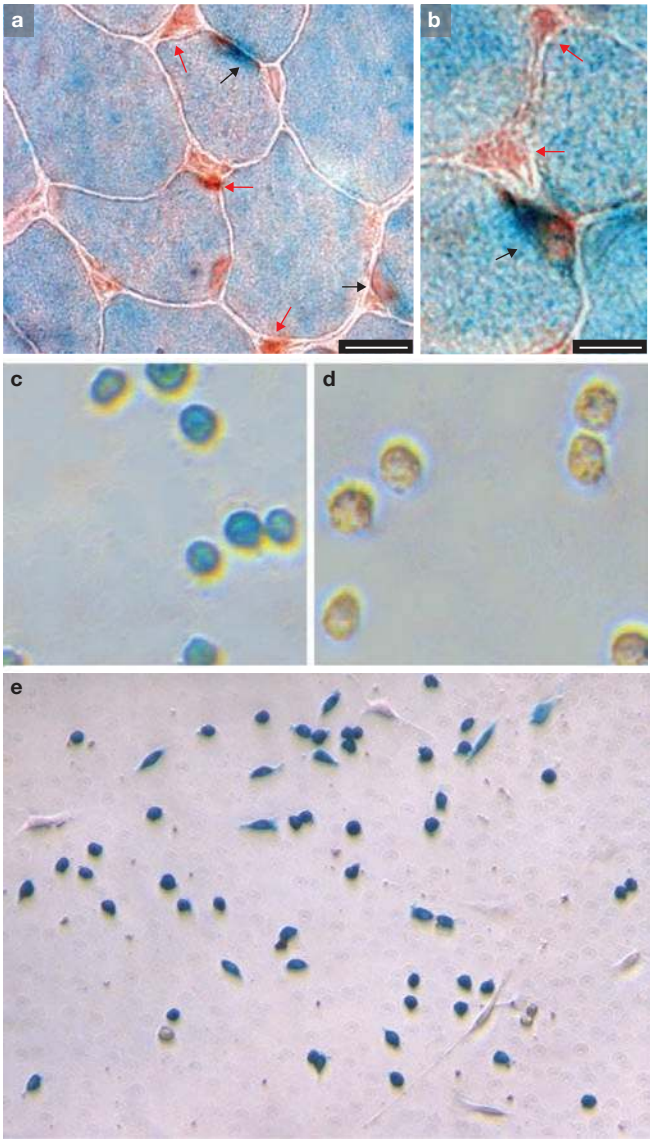

Figure 7 PICs are not derived from satellite cells. (**a**) Photomicrograph of a 2-week-old muscle from a *Pax3*$^{Cre/+}$ *X Rosa26*$^{LacZ/+}$ mouse. Sections were reacted with X-gal (blue) and stained for PW1 (brown). We note that all the muscle fibres and satellite cells (black arrows) are LacZ positive whereas no interstitial cells (red arrows) are positive for LacZ. Scale bar, 30 μm. (**b**) High resolution photomicrogaph of muscle as in **a**, showing a satellite cells marked by Pax3-Cre and stained for PW1 (black arrow). Interstitial cells positive for PW1 (PICs) are not marked by Pax3-Cre (red arrows). Scale bar, 10 μm. (**c**, **d**) Freshly isolated cytospun satellite cells (**c**) and PICs (**d**) were obtained from *Pax3*$^{Cre/+}$ X *Rosa26*$^{LacZ/+}$ crossed mice. Satellite cells are positive for β-galactosidase staining (**c**) whereas freshly isolated (cytospun) PICs are negative for β-galactosidase staining (**d**). (**e**) Colonies derived from freshly isolated PICs, as shown in **d**, and grown for several days in culture become positive for β-galactosidase staining.

fate outcomes with satellite cells (data not shown), suggesting that, unlike satellite cells, PICs are bipotent.

PICs are myogenically competent *in vivo* and participate in skeletal muscle regeneration

Evidence that satellite cells are muscle stem cells derives from studies demonstrating their potential to generate myofibres and satellite cells following muscle engraftment[2,13,45]. Therefore, we purified PICs from *Rosa26*$^{LacZ/+}$ mice or *β-actin–EGFP* mice to follow cell fate after injection into focally injured tibialis anterior muscles of nude mice. Freshly isolated satellite cells were injected into the contralateral limb tibialis anterior for direct comparison. We found that PICs participated as efficiently as satellite cells in myofibre formation, upon overall muscle inspection (Fig. 6a–c, i). However, PICs recolonized muscle tissue with less sharply defined boundaries compared with muscle recolonized by satellite cells (Fig. 6a, see inset, versus b). Histological examination of cross-sections of regenerated muscle following injection of labelled PICs revealed numerous labelled cells in the interstitium in all sections examined, whereas we did not observe labelled interstitial cells in muscle injected with satellite cells (Fig. 6c–e, j), suggesting PIC self-renewal. No labelled fibres or interstitial cells were observed in injured controlateral muscles that received an injection of PBS (data not shown). Close inspection of sectioned muscle injected with *R26*$^{LacZ/+}$ PICs revealed that PICs gave rise to Pax7^{+} satellite cells (Fig. 6f) as well as PW1^{+} interstitial cells (PICs; Fig. 6i). Satellite cell identity was further confirmed in regenerated muscle following injection with GFP-labelled PICs using antibodies against MCadherin and GFP (Fig. 6g). We found a significant contribution of PICs to their own compartment whereas no labelled PICs were generated following satellite cell injection (Fig. 6j). While PICs form smooth muscle *in vitro*, we primarily observed a contribution of injected PICs to myofibres *in vivo,* suggesting the tissue environment exerts a role in PIC specification.

PICs are not derived from satellite cells

PICs show myogenic regenerative capacity at levels comparable to satellite cells, suggesting a common cell lineage. Lineage analyses using *Pax3*^{Cre} mice crossed with *Rosa*^{lacZ} mice confirmed that all cells derived from Pax3-expressing cells are myofibres and satellite cells (Fig. 7a, b)[2,12,19]. In contrast, we did not observe Pax3-derived cells in the interstitium (Fig. 7a, b). PICs isolated from the *Pax3*^{Cre} × *Rosa*^{lacZ} mice contained almost no β-galactosidase-stained (blue) cells whereas satellite cells were blue (Fig. 7c, d). When PICs were cultured, we observed that all myogenic colonies were blue, demonstrating Pax3 expression upon entry of PICs into the skeletal muscle lineage (Fig. 7e). These data demonstrate that PICs are not derived from satellite cells.

DISCUSSION

Satellite cells are considered to be the main source of myonuclei in postnatal muscle[9,13,21,46]. However, the role of the satellite cell as a unique muscle progenitor has been challenged by reports of vascular or bone marrow cells with myogenic potential, as well as of resident multipotent stem cells[9,24,30,44,46–48]. As these cells do not express satellite cell markers (Pax7, MCadherin and NCAM) upon isolation, it is assumed that they lie outside the satellite cell niche. Defining a precise anatomical location for these progenitor cells has been challenging due to the lack of cellular markers, with the exception of Alp in the mesoangioblast/pericyte[30]. In this study, we provide evidence for muscle progenitors that are defined by their location in the interstitium coupled with PW1 expression. Similarly to satellite cells[17,49], this subpopulation of interstitial cells (PICs) is more abundant at birth and declines until about 2–3 weeks after birth, maintaining a 1:1 ratio with satellite cells. This decline in satellite cells may reflect recruitment to muscle during postnatal growth.

We demonstrated previously that PW1-expressing cells increase during regeneration, greatly exceeding the number of Pax7-positive cells[32];

however, their precise role during myogenesis was not defined. A key role for Pax7 was demonstrated by the observation that *Pax7*$^{-/-}$ mice show a dramatic decrease in satellite cells during postnatal growth[8,12,17,19]. We note that there is a pronounced increase in PICs before the decline in satellite cells, representing the earliest developmental muscle phenotype in the Pax7 constitutive mutant. *Pax7*$^{-/-}$ bulk muscle cultures are reported to have limited myogenic potential and to participate in non-muscle lineages such as fat and blood, suggesting a primary role for Pax7 in lineage specification[8,50]. Increased cell death has also been reported in Pax7 mutant satellite cells, suggesting a role for Pax7 in satellite cell maintenance[8,17]. Here, we report that purified Pax7 mutant satellite cells are myogenically competent, form normal-sized colonies and are able to form myotubes in culture. Although our studies do not address Pax7 mutant satellite cell capacity for self-renewal or other critical stem cell properties, we show a clear defect in the behaviour of Pax7-deficient PICs, which are not myogenic under any conditions tested.

The capacity of PICs to participate in myogenesis *in vivo* at levels comparable to those obtained with freshly isolated satellite cells, demonstrates that PICs are a significant myogenic progenitor population. However, only PICs give rise to more PICs in addition to satellite cells and myofibres. These data show that PICs re-populate their niche at high levels, fulfilling one criterion for stem cell self-renewal. In this regard, skeletal muscle may be comparable to other tissues, such as the skin, in which multipotent bulge stem cells give rise to specified populations of progenitors, including keratinocytes, which either remain quiescent or progress to form epidermis[51,52].

We show that PICs require *Pax7* for myogenic specification, a role originally proposed for this gene[8,20,38], which may have a critical role in postnatal muscle. The capacity for satellite cell self-renewal may not be sufficient until after postnatal growth is complete. This is consistent with a recent report confirming that Pax7 is required for postnatal muscle growth but not for adult muscle regeneration[22]. Whereas our lineage analyses confirm that satellite cells are derived from a Pax3 lineage[2,12,19], PICs express Pax3 during myogenic commitment. It remains to be determined whether PICs are a source of satellite cells during normal postnatal development.

PW1 was isolated from a screen designed to identify early stem cell compartments that give rise to the myogenic lineage[31]. PW1 protein associates with TRAF2, which acts as an adaptor in TNF signalling, leading to NFkB activation[34,37]. PW1 is also a p53-effector protein that associates with Bax and Siah1 in mediating cell death in non-muscle cells and can directly regulate myogenic differentiation through the caspase pathway[32,36,54–56]. It is striking that two muscle stem cell populations (satellite cells and PICs) constitutively express PW1, which may reflect a role in rapid and efficient recruitment after trauma and stress. □

METHODS

Methods and any associated references are available in the online version of the paper at http://www.nature.com/naturecellbiology/.

Note: Supplementary Information is available on the Nature Cell Biology website.

ACKNOWLEDGEMENTS

We gratefully thank F. Relaix for fruitful discussions and critical reading of the manuscript. We thank A. Galy, E. Negroni and L. Arandel for technical advice and C. Blanc (Cytométrie en Flux platform, Institut Fédératif de Recherche 113) for FACs assistance. This work was supported by a grant from the NIH (NCI PO1 CA80058-06, subproject 3), a French Ministry of Research 'Chaire d'Excellence' to D.S. and the Muscular Dystrophy Association of America to D.S. and E.R.G. K.M. is a recipient of an INSERM 'contrat de jeunes chercheurs'. B.C. is a recipient of a grant from Fondation pour la Recherche Médicale (FRM). E.R.G. is supported in part by the Inserm Avenir Program. This work benefited from funding from the European Community's Seventh Framework Programme project OPTISTEM (Optimization of stem cell therapy for degenerative epithelial and muscle diseases contract number Health-F5-2009-223098). The Myology Group is the beneficiary of a Strategic Plan Support from the Association Française contre les Myopathies (AFM) and is affiliated with the Institute of Myology/ Association Institut Myologie.

AUTHOR CONTRIBUTIONS

All authors designed research; K.J.M., A.P., B.C., A.P. and V.B. performed research; B.C., V.B. and E.R.G. contributed new reagents/analytic tools; all authors analysed data and K.J.M., G.M. and D.A.S. wrote the paper.

COMPETING FINANCIAL INTERESTS

The authors declare no competing financial interests.

Published online at http://www.nature.com/naturecellbiology/.
Reprints and permissions information is available online at http://npg.nature.com/reprintsandpermissions/.

1. Endo, T. Stem cells and plasticity of skeletal muscle cell differentiation: potential application to cell therapy for degenerative muscular diseases. *Regen Med.* **2,** 243–256 (2007).
2. Montarras, D. *et al.* Direct isolation of satellite cells for skeletal muscle regeneration. *Science* **309,** 2064–2067 (2005).
3. Chen, J. C. & Goldhamer, D. J. Skeletal muscle stem cells. *Reprod. Biol. Endocrinol.* **1,** 101 (2003).
4. Asakura, A. Stem cells in adult skeletal muscle. *Trends Cardiovasc. Med.* **13,** 123–128 (2003).
5. Bischoff, R. Regeneration of single skeletal muscle fibers in vitro. *Anat. Rec.* **182,** 215–235 (1975).
6. Peault, B. *et al.* Stem and progenitor cells in skeletal muscle development, maintenance, and therapy. *Mol. Ther.* **15,** 867–877 (2007).
7. Charge, S. B. & Rudnicki, M. A. Cellular and molecular regulation of muscle regeneration. *Physiol. Rev.* **84,** 209–238 (2004).
8. Seale, P. *et al.* Pax7 is required for the specification of myogenic satellite cells. *Cell* **102,** 777–786 (2000).
9. Collins, C. A. *et al.* Stem cell function, self-renewal, and behavioral heterogeneity of cells from the adult muscle satellite cell niche. *Cell* **122,** 289–301 (2005).
10. Bischoff, R. Proliferation of muscle satellite cells on intact myofibers in culture. *Dev. Biol.* **115,** 129–139 (1986).
11. Hill, M., Wernig, A. & Goldspink, G. Muscle satellite (stem) cell activation during local tissue injury and repair. *J. Anat.* **203,** 89–99 (2003).
12. Relaix, F., Rocancourt, D., Mansouri, A. & Buckingham, M. A Pax3/Pax7-dependent population of skeletal muscle progenitor cells. *Nature* **435,** 948–953 (2005).
13. Zammit, P. S., Partridge, T. A. & Yablonka-Reuveni, Z. The skeletal muscle satellite cell: the stem cell that came in from the cold. *J. Histochem. Cytochem.* **54,** 1177–1191 (2006).
14. Mauro, A. Satellite cell of skeletal muscle fibers. *J. Biophys. Biochem. Cytol.* **9,** 493–495 (1961).
15. Irintchev, A., Zeschnigk, M., Starzinski-Powitz, A. & Wernig, A. Expression pattern of M-cadherin in normal, denervated, and regenerating mouse muscles. *Dev. Dyn.* **199,** 326–337 (1994).
16. Gros, J., Manceau, M., Thome, V. & Marcelle, C. A common somitic origin for embryonic muscle progenitors and satellite cells. *Nature* **435,** 954–958 (2005).
17. Oustanina, S., Hause, G. & Braun, T. Pax7 directs postnatal renewal and propagation of myogenic satellite cells but not their specification. *EMBO J.* **23,** 3430–3439 (2004).
18. Kuang, S., Kuroda, K., Le Grand, F. & Rudnicki, M. A. Asymmetric self-renewal and commitment of satellite stem cells in muscle. *Cell* **129,** 999–1010 (2007).
19. Relaix, F. *et al.* Pax3 and Pax7 have distinct and overlapping functions in adult muscle progenitor cells. *J. Cell Biol.* **172,** 91–102 (2006).
20. Olguin, H. C. & Olwin, B. B. Pax-7 up-regulation inhibits myogenesis and cell cycle progression in satellite cells: a potential mechanism for self-renewal. *Dev. Biol.* **275,** 375–388 (2004).
21. Zammit, P. S. *et al.* Muscle satellite cells adopt divergent fates: a mechanism for self-renewal? *J. Cell Biol.* **166,** 347–357 (2004).
22. Lepper, C., Conway, S. J. & Fan, C. M. Adult satellite cells and embryonic muscle progenitors have distinct genetic requirements. *Nature* (2009).
23. Asakura, A., Seale, P., Girgis-Gabardo, A. & Rudnicki, M. A. Myogenic specification of side population cells in skeletal muscle. *J. Cell Biol.* **159,** 123–134 (2002).
24. De Angelis, L. *et al.* Skeletal myogenic progenitors originating from embryonic dorsal aorta coexpress endothelial and myogenic markers and contribute to postnatal muscle growth and regeneration. *J. Cell Biol.* **147,** 869–878 (1999).
25. LaBarge, M. A. & Blau, H. M. Biological progression from adult bone marrow to mononucleate muscle stem cell to multinucleate muscle fiber in response to injury. *Cell* **111,** 589–601 (2002).
26. Tamaki, T. *et al.* Skeletal Muscle-Derived CD34+/45- and CD34-/45- Stem Cells Are Situated Hierarchically Upstream of Pax7+ Cells. *Stem Cells Dev.* (2008).
27. Lee, J. Y. *et al.* Clonal isolation of muscle-derived cells capable of enhancing muscle regeneration and bone healing. *J. Cell Biol.* **150,** 1085–1100 (2000).

28. Torrente, Y. *et al.* Intraarterial injection of muscle-derived CD34(+)Sca-1(+) stem cells restores dystrophin in mdx mice. *J. Cell Biol.* **152,** 335–348 (2001).
29. Polesskaya, A., Seale, P. & Rudnicki, M. A. Wnt signaling induces the myogenic specification of resident CD45+ adult stem cells during muscle regeneration. *Cell* **113,** 841–852 (2003).
30. Dellavalle, A. *et al.* Pericytes of human skeletal muscle are myogenic precursors distinct from satellite cells. *Nature Cell Biol.* **9,** 255–267 (2007).
31. Relaix, F. *et al.* Pw1, a novel zinc finger gene implicated in the myogenic and neuronal lineages. *Dev. Biol.* **177,** 383–396 (1996).
32. Schwarzkopf, M., Coletti, D., Sassoon, D. & Marazzi, G. Muscle cachexia is regulated by a p53-PW1/Peg3-dependent pathway. *Genes Dev.* **20,** 3440–3452 (2006).
33. Nicolas, N., Marazzi, G., Kelley, K. & Sassoon, D. Embryonic deregulation of muscle stress signaling pathways leads to altered postnatal stem cell behavior and a failure in postnatal muscle growth. *Dev. Biol.* **281,** 171–183 (2005).
34. Coletti, D., Yang, E., Marazzi, G. & Sassoon, D. TNFalpha inhibits skeletal myogenesis through a PW1-dependent pathway by recruitment of caspase pathways. *Embo J.* **21,** 631–642 (2002).
35. Coletti, D., Moresi, V., Adamo, S., Molinaro, M. & Sassoon, D. *Tumor necrosis factor-alpha* gene transfer induces cachexia and inhibits muscle regeneration. *Genesis* **43,** 119–127 (2005).
36. Relaix, F. *et al.* Pw1/Peg3 is a potential cell death mediator and cooperates with Siah1a in p53-mediated apoptosis. *Proc. Natl Acad. Sci. U S. A* **97,** 2105–2110 (2000).
37. Relaix, F., Wei, X. J., Wu, X. & Sassoon, D. A. Peg3/Pw1 is an imprinted gene involved in the TNF-NFkappaB signal transduction pathway. *Nature Genet.* **18,** 287–291 (1998).
38. Seale, P., Ishibashi, J., Scime, A. & Rudnicki, M. A. Pax7 is necessary and sufficient for the myogenic specification of CD45+:Sca1+ stem cells from injured muscle. *PLoS Biol.* **2,** E130 (2004).
39. Moura-Neto, V. *et al.* A 28-bp negative element with multiple factor-binding activity controls expression of the vimentin-encoding gene. *Gene* **168,** 261–266 (1996).
40. Sax, C. M., Farrell, F. X. & Zehner, Z. E. Down-regulation of vimentin gene expression during myogenesis is controlled by a 5'-flanking sequence. *Gene* **78,** 235–242 (1989).
41. Ontell, M. & Kozeka, K. The organogenesis of murine striated muscle: a cytoarchitectural study. *Am. J. Anat.* **171,** 133–148 (1984).
42. Ontell, M., Hughes, D. & Bourke, D. Morphometric analysis of the developing mouse soleus muscle. *Am. J. Anat.* **181,** 279–288 (1988).
43. Hughes, D. S. & Ontell, M. Morphometric analysis of the developing, murine aneural soleus muscle. *Dev. Dyn.* **193,** 175–184 (1992).
44. Sherwood, R. I. *et al.* Isolation of adult mouse myogenic progenitors: functional heterogeneity of cells within and engrafting skeletal muscle. *Cell* **119,** 543–554 (2004).
45. Sacco, A., Doyonnas, R., Kraft, P., Vitorovic, S. & Blau, H. M. Self-renewal and expansion of single transplanted muscle stem cells. *Nature* **456,** 502–506 (2008).
46. Buckingham, M. *et al.* The formation of skeletal muscle: from somite to limb. *J. Anat.* **202,** 59–68 (2003).
47. Tamaki, T. *et al.* Identification of myogenic-endothelial progenitor cells in the interstitial spaces of skeletal muscle. *J. Cell Biol.* **157,** 571–577 (2002).
48. Tamaki, T., Akatsuka, A., Yoshimura, S., Roy., R. R. & Edgerton, V. R. New fiber formation in the interstitial spaces of rat skeletal muscle during postnatal growth. *J. Histochem. Cytochem.* **50,** 1097–1111 (2002).
49. Campion, D. R., Richardson, R. L., Kraeling, R. R. & Reagan, J. O. Changes in the satellite cell population in fetal pig skeletal muscle. *J. Anim. Sci.* **48,** 1109–1115 (1979).
50. Asakura, A., Komaki, M. & Rudnicki, M. Muscle satellite cells are multipotential stem cells that exhibit myogenic, osteogenic, and adipogenic differentiation. *Differentiation* **68,** 245–253 (2001).
51. Nowak, J. A., Polak, L., Pasolli, H. A. & Fuchs, E. Hair follicle stem cells are specified and function in early skin morphogenesis. *Cell Stem Cell* **3,** 33–43 (2008).
52. Fuchs, E. & Horsley, V. More than one way to skin. *Genes Dev.* **22,** 976–985 (2008).
53. Yamaguchi, A. *et al.* Peg3/Pw1 is involved in p53-mediated cell death pathway in brain ischemia/hypoxia. *J. Biol. Chem.* **277,** 623–629 (2002).
54. Johnson, M. D., Wu, X., Aithmitti, N. & Morrison, R. S. Peg3/Pw1 is a mediator between p53 and Bax in DNA damage-induced neuronal death. *J. Biol. Chem.* **277,** 23000–23007 (2002).
55. Deng, Y. & Wu, X. Peg3/Pw1 promotes p53-mediated apoptosis by inducing Bax translocation from cytosol to mitochondria. *Proc. Natl Acad. Sci. USA* **97,** 12050–12055 (2000).

METHODS

Mice. The animal models used were *Pax7* $^{+/+}$, *Pax7* $^{LacZ/+}$ and *Pax7* $^{LacZ/LacZ}$ C57Bl/6J mice[56], C57Bl6-*β-actin–EGFP* transgenic mice, in which cytoplasmic GFP is expressed ubiquitously under the control of the chicken β-actin promoter[57], *ROSA26 flox–LacZ*; *Pax3* $^{Cre/+}$, *PGK-Cre* mice (*R26LacZ*) and nu/nu mice (Elevage Janvier). All work with mice was carried out in adherence to French government guidelines.

Primary cell culture. Primary skeletal muscle cell cultures from the limb muscle of P10 mice were prepared by enzymatic digestion, as described previously[58]. Cells were plated on gelatin-coated dishes at a density of 1000 cells per cm^2 in BIOAMF-2 complete medium (ATGC). For myogenic differentiation, cells were transferred to differentiation medium (DM) for 24–36 h: DMEM (Gibco) containing 2% (v/v) horse serum (Gibco) and 1% (v/v) penicillin-streptomycin (Gibco).

FACS analysis. For fluorescence-activated cell sorting, limb muscles from 7–14-day-old *Pax7* $^{+/+}$, *Pax7* $^{LacZ/LacZ}$, i or *R26LacZ* mice were minced and digested in HBSS (GIBCO) containing 2 μg ml^{-1} collagenase A (Roche), 2.4 U ml^{-1} dispase I (Roche), 10 ng ml^{-1} DNAse I (Roche), 0.4 mM $CaCl_2$ and 5 mM $MgCl_2$ for 90–120 min at 37 °C with agitation every 15 min. Three successive cycles of washing and filtration were performed before re-suspension of the cell pellet in HBSS containing 0.2% (w/v) BSA (Sigma), 1% (v/v) penicillin-streptomycin, 10 ng ml^{-1} DNAse I and 10% (v/v) mouse serum (Jackson Immunoresearch). Cells were incubated for 5 min on ice before adding the following primary antibodies at a concentration of 10 ng ml^{-1}: rat anti-mouse CD34-biotin (Ram34; eBiosciences), rat anti-mouse CD45-APC (BD Biosciences), rat anti-mouse Ter119-APC or Ter119-PE (BD Biosciences) and rat anti-mouse Sca1-FITC or Sca1-PE (BD Biosciences). Cells were incubated for 30 min on ice. Cell pellets were washed before incubation with streptavidin-PE-Cy7 (1/500; BD Biosciences) for 30 min on ice. Cells were finally washed, filtered and re-suspended in HBSS containing 0.2% (w/v) BSA and 1% (v/v) penicillin-streptomycin. Flow cytometry analysis and cell sorting were performed on a FACSAria (Becton Dickinson), with appropriate isotype matching controls. $Ter119_{HIGH}$ and $CD45^+$ cells were gated and excluded by negative selection. The remaining cells were then gated and sorted based on their CD34 and Sca1 expression. Purified cell populations were cultured as described above. For immuncytochemical analyses, freshly sorted cells (10,000 cells per slide) were immediately centrifuged onto glass slides using a Cytospin (ThermoFisher Scientific) for 5 min at 1000 rpm and immunostained for PW1 and Pax7, as described below. Quantitative analyses were performed by counting the number of positive cells out of a minimum of 300 cells in randomly chosen fields for each of three independent experiments.

Tissue injury and transplantation. Skeletal muscle regeneration was induced by a focal freeze-crush injury of the tibialis anterior of 2 month-old female nu/nu mice, as described previously[59]. At 24 h post-injury, freshly isolated PICs ($CD34^+$ $Sca1_{MED}$ $CD45^-$ $Ter119_{HIGH}$) and satellite cells ($CD34^+$ $Sca1^-$ $CD45^-$ $Ter119_{HIGH}$) from hind- and forelimb muscles of 7–10-day-old *β-actin–EGFP* or *R26LacZ* mice were washed, re-suspended in PBS and directly injected into the damaged muscle (10,000–15,000 cells per tibialis anterior). As a control, injured tibialis anterior muscles were injected with PBS. Muscles were collected 14 days post-injection.

Histological analyses. For immunofluorescence and immunohistochemistry experiments, entire hindlimbs from 0–14-day-old *Pax7* $^{+/+}$, *Pax7* $^{LacZ/+}$, *Pax7* $^{LacZ/LacZ}$ and *Pax3* $^{Cre/+}$ *X Rosa26* $^{LacZ/+}$ mice and tibialis anterior muscles from transplanted nu/nu mice were snap frozen in liquid nitrogen-cooled isopentane or directly in liquid nitrogen. β-Galactosidase activity in *R26LacZ*-transplanted tibialis anterior muscles and *Pax3* $^{Cre/+}$ *X Rosa26* $^{LacZ/+}$ mice was revealed either before freezing or on transverse cryosections using X-gal, as described previously[10]. Cryosections (10 μ), cultured cells and cytospin preparations were fixed in 4% (w/v) paraformaldehye and processed for immunostaining as described previously[32–34]. Primary antibodies used were against: PW1 (ref. 31; 1:4,000), Pax7 (Developmental Studies Hybridoma Bank; 1:20), laminin (Sigma; 1:100), MCadherin (NanoTools; 1:100), Ki67 (BD Biosciences; 1:100), myoD (BD Biosciences; 1:100), smooth muscle actin (Sigma; 1:300), MF20 (Developmental Studies Hybridoma Bank; 1:2), GFP (Biovalley and Abcam; 1:400), Pecam-1 (BD Biosciences; 1:500), vimentin (Progene; 1:500) and F4/80 (AbCam; 1:500). For immunofluorescence, antibody binding was revealed using species-specific secondary antibodies coupled to Alexa Fluor 488 (Molecular Probes), Cy3 or Cy5 (Jackson Immunoresearch). As described previously[6], nuclei were counterstained with DAPI (Sigma). For immunohistochemistry, antibody binding was revealed using species-specific secondary antibodies coupled with horseraddish peroxidase (Jackson Immunoresearch) and the enzymatic reaction was performed according to the manufacturer's instructions (VECTOR NovaRED substrate kit, AbCys). For quantitative analyses of immunostained tissue, positive cells in at least 350 fibres from randomly chosen fields were counted from three animals for each age per genotype. Cells in culture were quantified by counting at least 400 cells from randomly chosen fields for each of three independent experiments. Fusion indexes were quantified by counting the number of nuclei in $MF20^+$ cells per total number of nuclei. For quantitative analysis of *R26LacZ* PICs and satellite cells, injected tibialis anterior muscles, blue fibres and interstitial cells from fields of the area of regeneration were counted from four animals for each experimental condition and were normalized to the fibre number in areas counted. At least 200 fibres (positive and negative) for each independent experiment were counted. Values represent the mean ± s.em. and statistical analyses were performed using Student's *t*-test, $*P < 0.05$, $**P < 0.01$ and $***P < 0.001$.

Microscopy and live-cell imaging. Images were acquired using a Leica DM-IL inverted fluorescence microscope, Leica DM fluorescence microscope or Leica SPE confocal microscope. For detection of GFP^+ myofibres, a narrow range of emission wavelength (511–532 nm) was used to avoid detection of autofluorescence[61].

For live-cell imaging, cell cultures were monitored using a Nikon Ti microscope equipped with an incubator to maintain cultures at 37 °C and 5% CO_2 (Okolab), a CoolSNAP HQ 2 camera (Roper Scientific) and an XY motorized stage (Nikon), driven by metamorph software (Molecular Devices). For myogenicity of the PICs, fluorescence (GFP) and phase contrast images were acquired every 10 min. For cell lineage, isolated PICs were plated on gelatin-coated dishes with custom-made 5-mm diameter silicon wells (sylgard 184, Dow Corning), to allow the observation of all the area of the well, using the XY stage. Cells were transferred just after plating to the microscope and images of the whole well were acquired every 12 or 30 min during 4 or 5 days. Cells were plated at a density of 1000 cells per cm2 in BIOAMF-2 complete medium (ATGC) for 3 or 4 days and then transferred to DMEM (Gibco) containing 2% (v/v) horse serum (Gibco) and 1% (v/v) penicillin-streptomycin (Gibco) for myogenic differentiation (1 day). Cells were fixed in 4% (w/v) paraformaldehyde immediately after the acquisition of the last image, permeabilized with cold methanol and blocked with 4% (w/v) BSA in PBS. Cells were immunostained using primary antibodies against smooth muscle actin (Sigma), MHCfast (AbCys), SM22a (AbCam) and MyoD (BD Biosciences) followed by secondary antibodies coupled to Cy3 or Cy5 (Jackson Immunoresearch). Nuclei were counterstained with DAPI (Sigma). Only wells containing one single cell at day 0 were analysed.

56. Mansouri, A., Stoykova, A., Torres, M. & Gruss, P. Dysgenesis of cephalic neural crest derivatives in Pax7-/- mutant mice. *Development* **122,** 831–838 (1996).
57. Wright, D. E. *et al.* Cyclophosphamide/granulocyte colony-stimulating factor causes selective mobilization of bone marrow hematopoietic stem cells into the blood after M phase of the cell cycle. *Blood* **97,** 2278–2285 (2001).
58. Montarras, D., Lindon, C., Pinset, C. & Domeyne, P. Cultured myf5 null and myoD null muscle precursor cells display distinct growth defects. *Biol. Cell* **92,** 565–572 (2000).
59. McGeachie, J. K. & Grounds, M. D. Initiation and duration of muscle precursor replication after mild and severe injury to skeletal muscle of mice. An autoradiographic study. *Cell Tissue Res.* **248,** 125–130 (1987).
60. Sanes, J. R., Rubenstein, J. L. & Nicolas, J. F. Use of a recombinant retrovirus to study post-implantation cell lineage in mouse embryos. *EMBO J.* **5,** 3133–3142 (1986).
61. Jackson, K. A., Snyder, D. S. & Goodell, M. A. Skeletal muscle fiber-specific green autofluorescence: potential for stem cell engraftment artifacts. *Stem Cells* **22,** 180–187 (2004).

nature cell biology

DOI: 10.1038/ncb2025

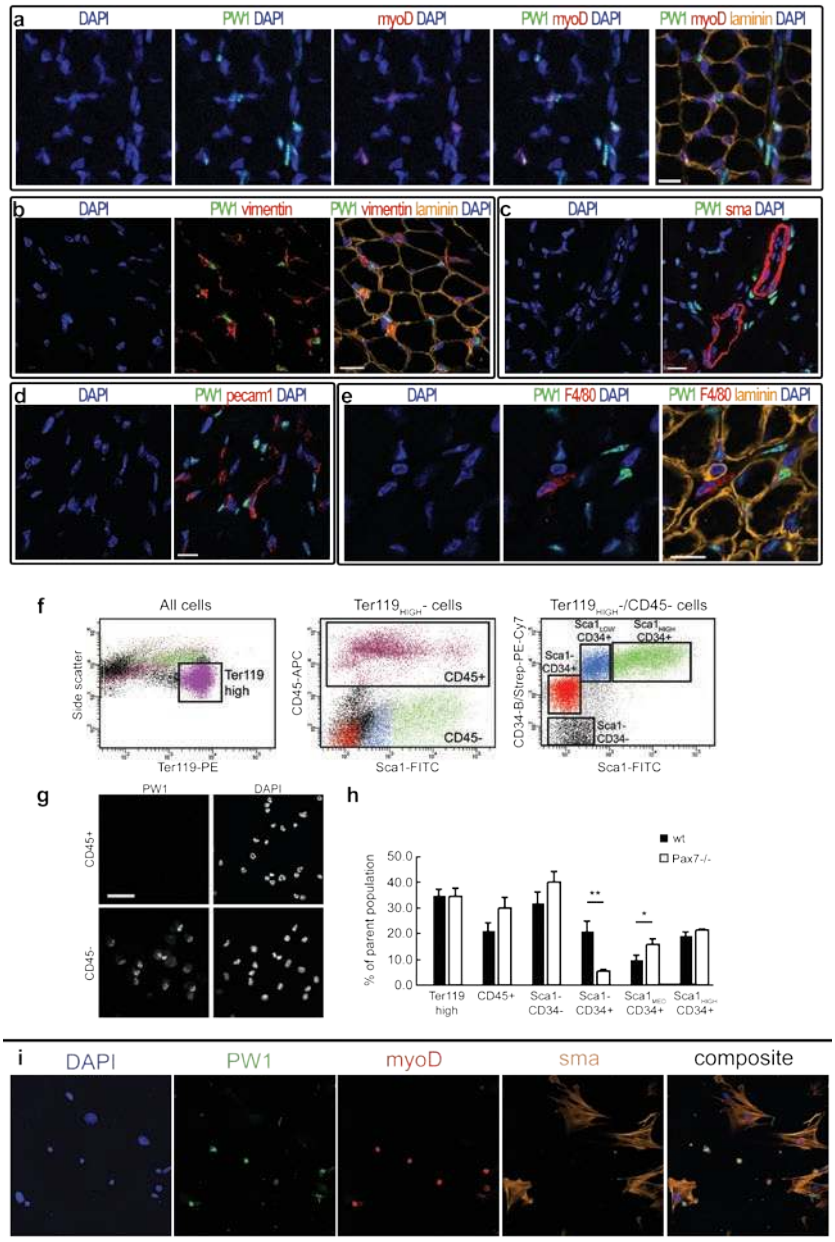

Figure S1 a-e. PICs are negative for markers of skeletal muscle, smooth muscle, endothelial cells and macrophages. Cross-sections of wildtype hindlimb muscle at P14 (**a**-**d**) or P2 (**e**), immunostained as indicated in the figure. Nuclei are visualized with DAPI. Scale bars = 50 μm. (**a**) MyoD+/PW1+ cells are observed underneath the basal lamina. PICs are negative for MyoD. (**b**) PICs express the intermediate filament vimentin. (**c**, **d**) PICs are often closely associated with vessels but PW1 (green) does not colocalise with either smooth muscle actin (red) (**c**) or the endothelial marker CD31/pecam1 (red) (**d**). (**e**) PICs are negative for the macrophage marker F4/80 (red). **f-h.** Isolation of muscle-resident populations by FACS using stem cell markers. (**f**) FACS profiles of single cells from P10 wildtype hindlimb muscles stained with antibodies against Ter119, CD45, Sca1 and CD34. $Ter119_{HIGH}$ cells were negatively selected to exclude erythrocytes (left panel). All CD45+ cells were negatively selected (middle panel). Ter119-/CD45- cells were then separated on the basis of Sca1 and CD34 expression (right panel). The gates used to isolate Sca1-/CD34-, Sca1-/CD34+, $Sca1_{MED}$/CD34+ and $Sca1_{HIGH}$/CD34+ cells are shown. (**g**) Representative photomicrographs of freshly sorted CD45+ and CD45- cells immunostained with PW1. Nuclei were counterstained with DAPI. PW1+ cells are only present in the CD45- population. Scale bar = 30 μm. (**h**) Quantification of % of cells in each population for P10 wildtype (black columns) and Pax7 -/- (open columns) hindlimb muscles. Pax7 -/- muscle has fewer Sca1-/CD34+ cells and more $Sca1_{MED}$/CD34+ cells. No significant differences were observed in the sizes of all other fractions. Values represent the mean % ± SEM (from 4 independent experiments) of positive cells from the following parent populations: all cells for $Ter119_{HIGH}$; Ter119- cells for CD45; and Ter119-/CD45- for the Sca1/CD34 fractions. **i.** Smooth muscle actin positive cells (sma) do not express skeletal muscle myoblast markers. Immunolocalisation of PW1 (green), MyoD (red), and smooth muscle actin (sma; orange) in PICs cultured for 4 days in growth media (differentiating). Nuclei were counterstained with DAPI. Only the smooth muscle actin negative cells are positive for MyoD and PW1.

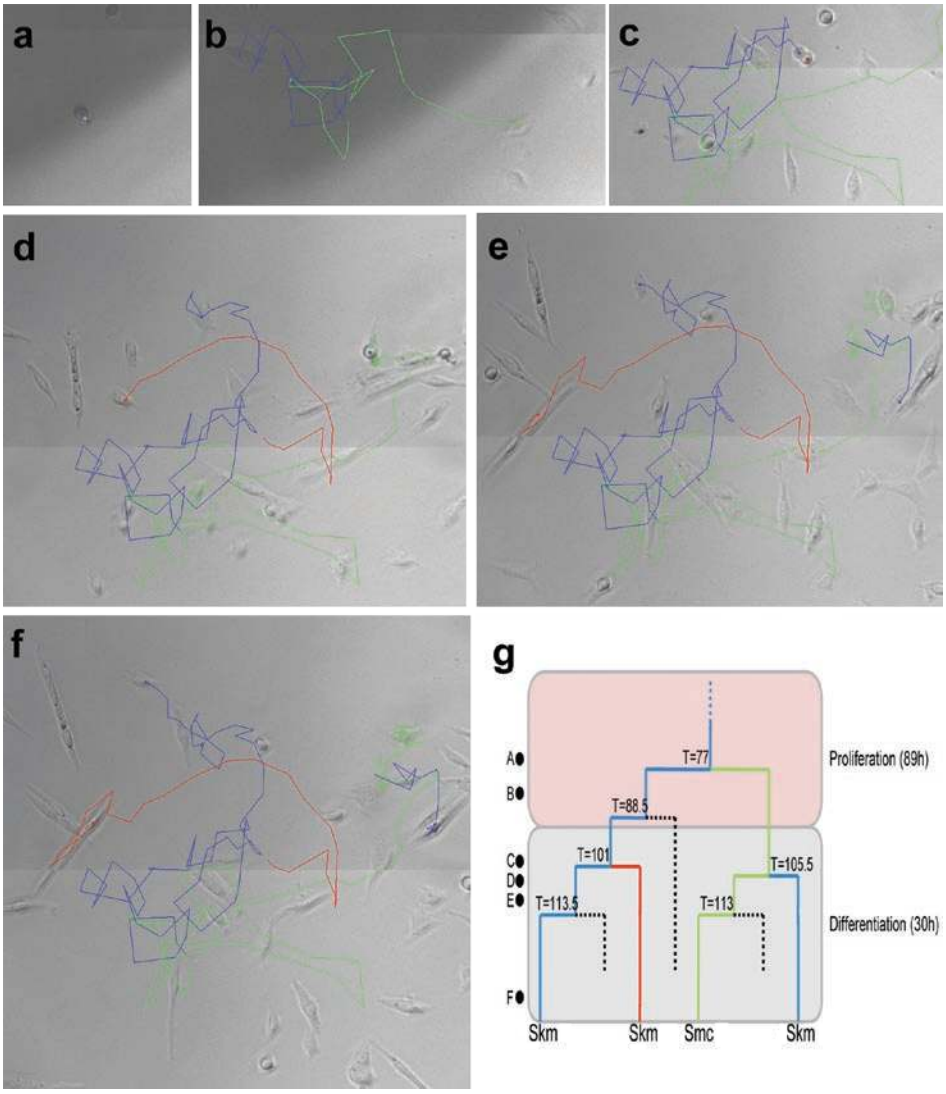

Figure S2 A geneology tree of a single PIC giving rise to smooth and skeletal muscle. (**a**-**f**) Representative frames from a time-lapse recording of freshly isolated PICs. Images were acquired over a 4 day period in growth medium (**a**-**b**) and 30 hours in differentiating medium (**c**-**f**). The parental cell shown in panel (**a**) divides several times (**a**-**d**) and coloured lines represent the divisions and movements of 4 cells derived from the initial cell. (**g**) Genealogy tree of the cell in the first frame (**a**) showing division time, colour-coded as shown in panels (**a**-**f**). The letters at the left correspond to the frames depicted in panels a-f and the time of cell divisions are indicated on the tree. The cell fates were determined by immunofluorescence staining as shown in Figure 5 (Skm-skeletal muscle, Smc-smooth muscle).

Supplementary Movie Legends

Movie 1 Real-time visualization of PICs contributing to myogenesis *in vitro*. Time-lapse recording of co-cultures of wildtype GFP-labelled PICs (green) and wildtype unlabeled satellite cells. Arrows indicate events during which a GFP-labelled PIC fuses with wildtype unlabeled satellite cells or myotubes. Frames from this movie are shown in Figure 4.

Movie 2 Real time visualization of cells shown in Figure 5. Real time lapse recording of entire cell history shown in Figure 5.